

ELECTRON BEAM WELDING WITH PROGRAMMING OF BEAM POWER DENSITY DISTRIBUTION

V.V. Skryabinskyi, V.M. Nesterenkov and M.O. Rusynyk

E.O. Paton Electric Welding Institute of the NAS of Ukraine

11 Kazymyr Malevych Str., 03150, Kyiv, Ukraine. E-mail: office@paton.kiev.ua

In the existing models of electron beam welding process, the shape and size of penetration zone are determined both by energy parameters and shape of the heat source. Effective control of electron beam power density distribution and, therefore, of the heat source shape is possible by using discrete scans. A procedure and computer program were developed to calculate the power density distribution at discrete scanning of the electron beam, taking into account the coordinates of scan points, relative time of its dwelling in the points and scanning frequency. Joint application of the computer program for calculation of beam power density distribution together with the mathematical model of electron beam welding allows obtaining the set shape and dimensions of the penetration zone. The results of calculation of welding modes and cross-sections of welds with parallel side walls and a large radius of the root rounding at partial penetration of stainless steel samples are presented. The method of calculation of electron beam welding parameters and cross-section of the joint of dissimilar alloys are also given. 11 Ref., 7 Figures.

Keywords: electron beam welding, beam power density, computer-aided design of scans, shape of penetration zone, welding of dissimilar alloys

In electron beam welding (EBW) accelerating voltage, beam current, welding speed and beam focal spot position relative to the surface of the item being welded are the main parameters of the mode. In case of application of beam oscillations, the pattern, amplitude and frequency of scanning are added to them. Simultaneous accounting for EBW parameters, in order to produce high quality joints is a complicated but urgent task.

The objective of this work is demonstration of the possibility of controlling the vapour-gas channel shape, and, accordingly, shape of penetration zone, using computer design of beam scan patterns with simultaneous application of EBW mathematical model.

Intensity of electron beam impact in any point of the treated surface is proportional to its power density. Many researchers call the ability to change the electron beam power density distribution the main effect of scanning (here and furtheron, we mean not the instantaneous, but averaged over the scanning period beam power density). Here, the shape of vapour-gas channel, its resistance to external disturbances, penetration zone shape and, accordingly, the probability of root defect formation are changed [1–4].

The distribution of electron beam power density and, hence, the heat source shape in EBW, can be efficiently controlled using digital scanning systems [5, 6]. In such systems, the electron beam moves discretely by a given matrix of points that make up the scanning pattern. The coordinates of the pattern points and

relative time of beam dwelling in these points over one period of scanning are saved in a read only memory (ROM). The control system converts the digital scan code into electric signals and feeds them to the electron beam gun deflection coils.

Assessment of electron beam power density distribution is a rather complex task, even when using the simplest scan patterns (circle, semicircle, etc.). Here, alongside the pattern, it is also necessary to take into account the degree of beam focusing and scan amplitude along axes X and Y . When using discrete scans, the calculation formula also includes the coordinates of beam dwelling points and relative duration of its dwelling. In connection with the fact that beam transition from one point to another one is performed at a final speed (that is determined by the total inertia of the deflection system), beam power distribution density will be determined also by scan frequency [7].

Assuming the density distribution in a static beam close to a Gaussian one, the relative density of the scanning electron beam power in i -th point $q(x_i, y_i)$ can be determined as the sum of impact N of normal point and N linear sources:

$$q(x_i, y_i) = \sum_{j=1}^N \exp\left(-\frac{r_{ij}^2}{2r_e^2}\right) t_j + A(f) = \sum_{j=1}^N \exp\left(-\frac{r_{ik}^2}{2r_e^2}\right) t_{j(j-1)}, \quad (1)$$

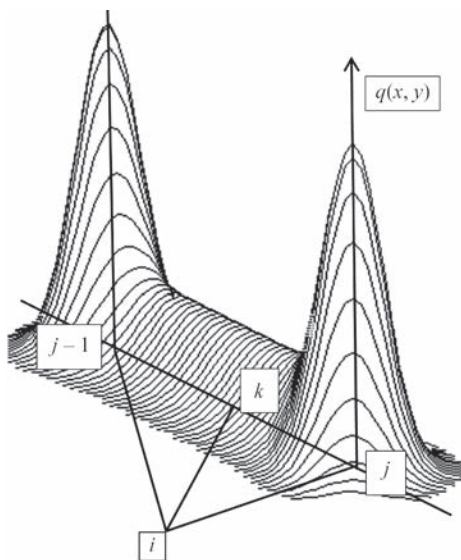


Figure 1. Scheme for calculation of electron beam power density distribution taking into account the scanning frequency

where $A(f)$ is the ratio of the intensity of the point and linear sources, dependent on scan frequency (f); N is the number of scan points; r_e is the effective beam radius; r_{ij} is the distance from calculated point i to j -th point of the scan; r_{ik} is the distance from calculated point i to the linear source; t_j is the relative time of the beam dwelling in the j -th point of the scan; $t_{j(j-1)}$ is the time of the beam transition from $j-1$ point into point j .

The calculation schematic is shown in Figure 1. Function $A(f)$ is calculated by numerical methods, taking into account the total inertia of beam deflection system. In our case system inertia depends on the parameters of deflection coils, scan generator and deflecting current amplifiers.

Computer programs for scan design and operative control of beam power density distribution at EBW allow performing highly accurate calculations

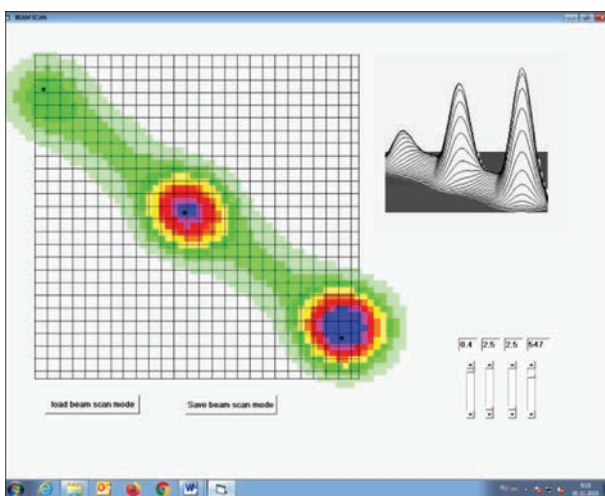


Figure 2. Heat source shape (horizontal projection and 3D image) when designing the scan pattern on the computer screen. Scan parameters; point number — 3; relative time of beam dwelling in points 1, 2, 3; frequency — 550 Hz

and displaying and/or saving the obtained results in the ROM [7, 8]. When designing the scans, the user assigns coordinates N of discrete beam positions, as well as the time of its dwelling in each of the selected positions (Figure 2).

At the same time, the computer screen displays the shape of the heat source (horizontal projection and 3D image). There is a capability of freely dragging the scan points over the screen or loading from ROM and editing the already existing patterns. It is important to note that during the design stage the user not only places the scan pattern points and assigns the relative time of beam dwelling, but he can also check the impact of the change of focusing, amplitude and frequency of scanning on the resultant distribution of beam power.

Each of these parameters has its specific impact on the result of calculation by formula (1) and, therefore, on EBW process. In order to clarify this impact, a computer program was used to conduct calculations of the given distributions of beam power at alternate change of scan amplitude (D), degree of focusing (beam effective radius r_e) and beam dwell time (T) in the scan points (Figure 3).

Calculations were conducted for a circular scan pattern. Increase of scan amplitude leads to proportional increase of the width of beam impact zone at an abrupt lowering of its intensity and formation of a depression in the central part of the graph. Beam defocusing (r_e increase) also increases the width of the impact zone, leveling the central depression in the graph. Change of the time of beam dwelling in the scan pattern points allows controlling in a broad range the distribution of power density, practically not affecting its width. So, the heat input in the weld central part can be changed two times, by shifting the points with doubled beam dwell time from the central to side parts of the weld pool as shown in Figure 4.

Where and how can the computer control of electron beam power density distribution be used? Information on the heat source shape may be needed for further calculations, related to mathematical modeling of EBW process. For instance, control of the penetration zone shape and dimensions has always been an urgent task, in terms of both EBW theory and practice. A number of existing models of EBW process not only allow assessing the weld depth and width, but also calculate the penetration zone shape. In them the capability of regulation of energy distribution in the heat source during calculations is not envisaged, and the main conclusions usually concern the degree of conformity of the calculated and experimental data [9–11].

Programming of the distribution of beam power density allows changing the heat source shape in a broad range, and, thus, it is a convenient tool for con-

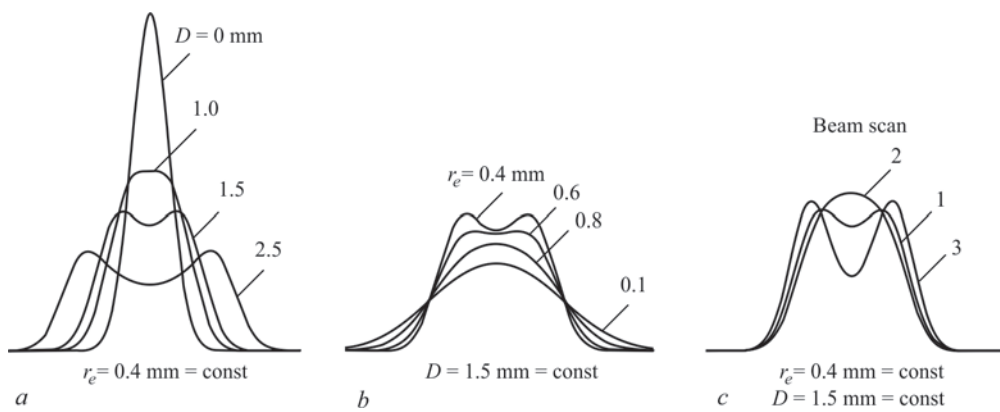


Figure 3. Distribution of electron beam power density for a circular scan at the change of: circular scan amplitude (*a*); beam focusing (*b*); relative time of beam dwelling in scan pattern points (*c*). Beam scans for calculation of the curves in Figure 3 are shown in Figure 4

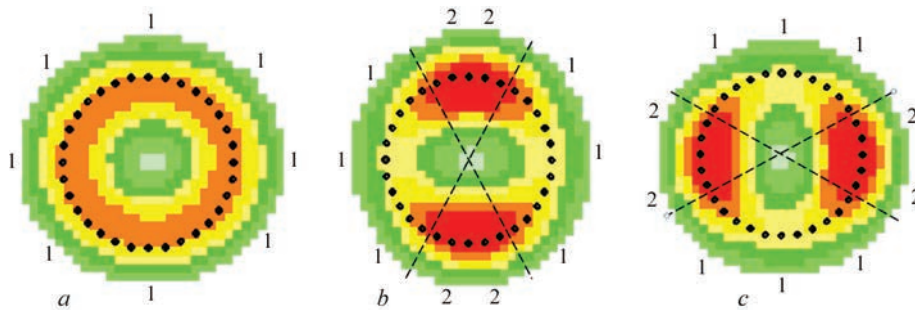


Figure 4. Circular patterns of the electron beam (32 points) with different relative time of beam dwelling in the scan pattern points. Numbers in the figure indicate the relative time of beam dwelling in the points: *a* — beam scan 1; *b* — 2; *c* — 3

trolling the penetration zone shape. Of practical interest was introduction of a variable (in our case beam power density distribution) into the mathematical model, changing which allows controlling the penetration zone shape.

In this work the mathematical model presented in [3] was selected for prediction of the penetration zone shape. In it the law of energy conservation is used as a base for deriving an equation for an element of the penetration channel surface, which describes the shape of the channel front wall in a cylindrical system of coordinates for any distribution of electron beam power density:

$$\frac{dr}{dz} = \frac{\rho V_w G \cos \varphi - q_{h,r}}{\eta}, \quad (2)$$

where ρ is the specific weight of metal; V_w is the welding speed; G is the heat content in a unit of metal mass; $q_{h,r}$ — heat removal power density; η is the effective efficiency of the process; $q(r, \varphi)$ is the beam power density distribution.

Practical verification of the method to control the penetration zone formation was performed as follows. The computer program for calculation of the distribution of electron beam power density by formula (1) was complemented by the equation of penetration channel (2) and the image of the channel front wall was displayed. The penetration zone shape was calculated for EBW of stainless steel with partial pene-

tration in the following mode: accelerating voltage of 60 V; beam current of 170 A; welding speed of 10 m/s; discrete circular scan of the beam (point number $N = 32$) with 1.5 mm amplitude, 500 Hz frequency and uniform heat input along the beam path. Considering the relatively low heat conductivity of the material, it was decided to ignore the losses for heat removal from the front wall of the penetration channel. Scan patterns, distribution of beam power density, calculated and experimental shapes of the penetration zone are shown in Figures 5, 6.

The above-given mode was used for welding a test sample from stainless steel and macrosection 1 was prepared (Figure 6, *b*). Calculated and experimental geometrical characteristics of the penetration zone differed only slightly. The weld width was about 2.0 mm at 24 mm penetration depth. The weld root was sharp. It is known that with such a shape of the penetration zone, weld formation is often accompanied by root defects in the form of voids unfilled by metal.

Energy distribution in the heated spot was changed, increasing the relative time of the beam dwelling in the points of the circular scan pattern, in the side parts of the weld pool. The number of points, their coordinates and other parameters of EBW mode remained unchanged. At each change of the dwell time (as of any other parameter) the computer program reflected the respective changes of beam power density distribution and penetration zone shape. After a certain

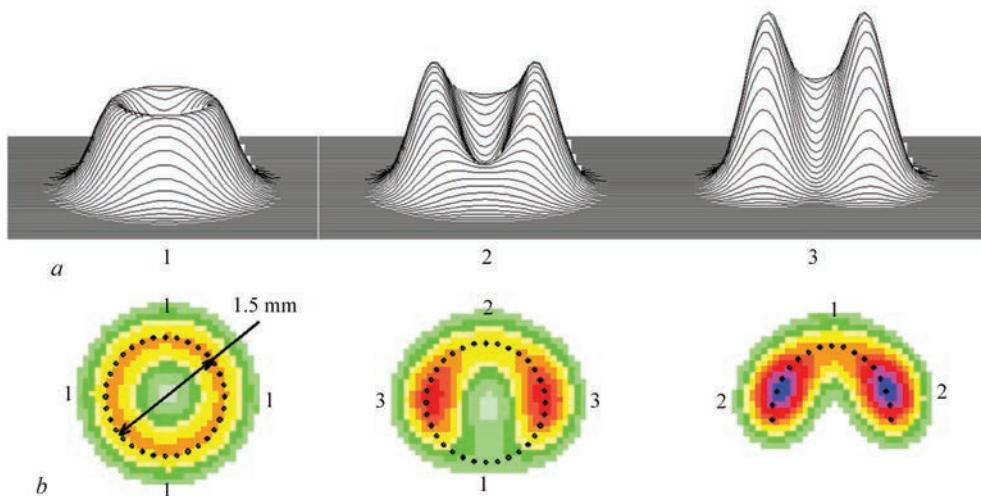


Figure 5. Distribution of electron beam power (*a*) and scan pattern (*b*) at EBW of stainless steel (for description of 1–3 see the text)

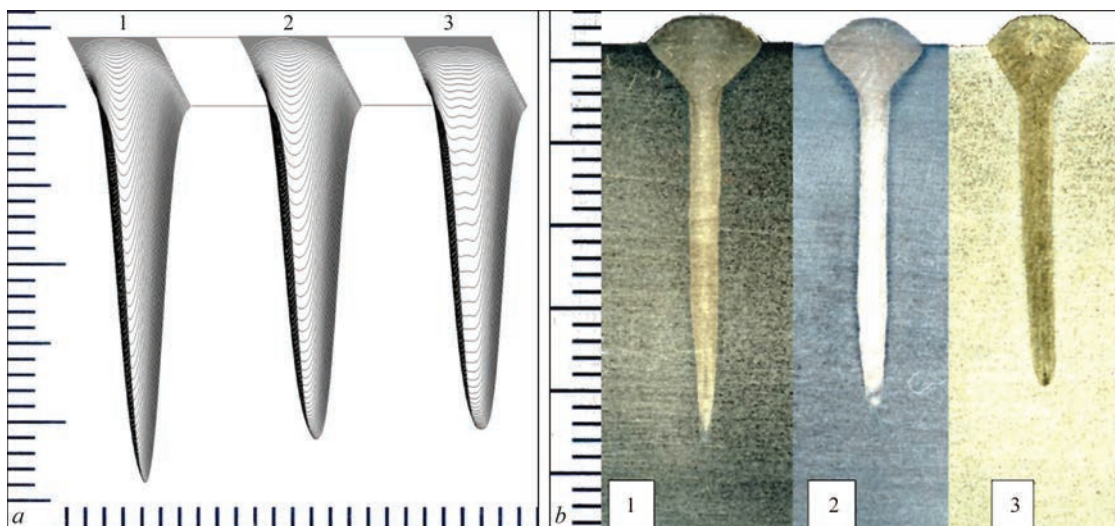


Figure 6. Calculated shape of penetration channel front wall (*a*) and transverse sections (*b*) at EBW of stainless steel (for description of 1–3 see the text)

shifting of heating from weld axis to weld pool side parts, we increased the rounding radius of the weld root approximately two times. The penetration depth here decreased from 24 to 22 mm (see Figure 6, *a* — 2). Beam scan parameters were stored in the ROM.

Similarly, a computer program was used to design the electron beam scan pattern in the form of a semi-circle. That is, first the beam dwell points were placed at equal distance from each other in the selected scan pattern (in our case, along an arc of a circle with beam reciprocal movement) on the screen. Then, EBW mode parameters, characteristics of the material being welded were entered into the program, and a computer image of the penetration zone shape was shown on the screen. Similar to the previous case, gradually increasing the relative time of beam dwelling in the side parts of the scan pattern, we tried to achieve a maximum increase of the rounding radius in the weld root (see Figure 6, *a*, — 3). EBW mode, including the designed beam scans, was used in EBW of stainless

steel vacuum chambers. Ultrasonic testing of welded joints showed absence of lacks-of-fusion or root defects along the entire weld length.

Computer design of electron beam scans can be useful at EBW of dissimilar metals. A usual technique in welding dissimilar metals and alloys is shifting the axially symmetrical heated spot towards the more refractory metal. The value of this displacement is either calculated, or determined experimentally. Thus, the probability of formation of lacks-of-fusion in the weld root part is reduced.

In EBW with programming of beam power density, it is necessary to increase the heat input into the refractory metal, while controlling the scan parameters. Thermo-physical calculations are based on the fact that the ratio of powers of the beam which falls on the edges should be proportional to the ratio of the quantity of heat, required for melting a unit of volume of each metal. Part of electron beam power consumed in heating metal 1, can be calculated by the following formula:

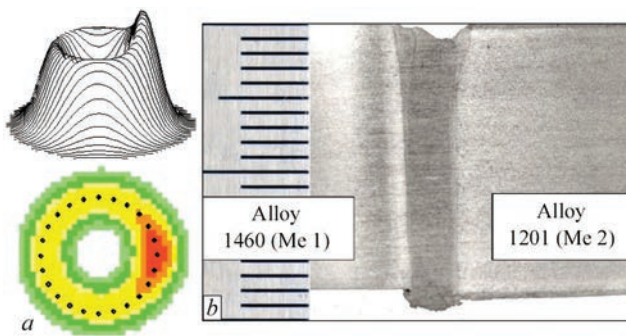


Figure 7. Scan pattern with electron beam power density distribution (a) and weld cross-section (b) at EBW of alloys 1460 and 1201

$$Q_{Me1} = 0.24\eta I_b U_{acc} \iint_{Me1} q(x, y) dx dy, \quad (3)$$

where η is the effective efficiency of the process; I_b is the beam current; U_{acc} is the accelerating voltage; $Me1$ is the area of beam impact, which falls on metal 1; $q(x, y)$ is the distribution of beam power density.

Beam power for metal 2 is calculated similarly. Thus, controlling the power density distribution between the different areas of beam impact, we can create the conditions for formation of a symmetrical shape of the penetration zone.

The method of EBW of dissimilar alloys with regulation of the heat input was realized in welding samples from aluminium alloys 1201 (Al–Cu alloying system) and 1460 (Al–Cu–Li alloying system) 18 mm thick. Thermophysical calculation showed that for simultaneous melting of equal amounts of metal of these alloys it is necessary to direct approximately 55 % of electron beam power to the edge of alloy 1201 and approximately 45 % of power to alloy 1460. Welding was performed with circular scanning of the beam with 2.5 mm amplitude. Selection of beam scan parameters to provide the required shifting of beam power towards alloy 1201 was conducted using a computer program. Calculations by formula (3) were easy to perform, so that the information on electron beam power density $q(x, y)$ is written in the form of a two-dimensional file in the program, which is not difficult to integrate (sum up) for any area.

Welding was performed using accelerating voltage of 30 kV and beam current of 350 mA at the speed of 11 mm/s. Beam power density distribution and penetration zone cross-section are shown in Figure 7.

The weld side walls are practically parallel, and X-ray spectral analysis of different areas of the welded joint showed that the alloying element content in

the weld metal fluctuates around the arithmetic mean of their content in the alloys being welded. This is indicative of the fact that at surface melting both the butt edges were equally involved in weld formation.

Conclusions

1. Computer design of beam scans with simultaneous application of EBW mathematical model enables controlling the shape of the vapour-gas channel, and, hence, the penetration zone shape.
2. Controlling the distribution of beam power density allows welding dissimilar metals and alloys with formation of a symmetrical penetration zone.

1. Ryzhkov, F.N., Suvorin, V.Ya. (1971) Technological features of vacuum welding by electron beam oscillating across the weld. *Avtomatich. Svarka*, **1**, 16–21 [in Russian].
2. Nesterenkov, V.M., Kravchuk, L.A. (1981) Selection of parameters of beam rotation around the circumference and their influence on weld geometry in electron beam welding. *Ibid.*, **10**, 25–28 [in Russian].
3. Nazarenko, O.K., Kaydalov, A.A., Kovbasenko, S.M. (1987) *Electron beam welding*. Ed. by B.E. Paton. Kiev, Naukova Dumka [in Russian].
4. Varushkin, S.V., Belenky, V.Ya., Zyryanov, N.A., Kylosov, A.A. (2017) Oscillation of electron beam as a means of improvement of weld root formation and facilitation of through penetration in electron beam welding. *Mashinostroenie, Materialovedenie*, **19(2)**, 151–159 [in Russian].
5. Lankin, Yu.N., Bondarev, A.A., Bajshtruk, E.N., Skryabinsky, V.V. (1985) Control of density distribution of electron beam power over its section. *Avtomatich. Svarka*, **6**, 12–15 [in Russian].
6. Lankin, Yu.N., Bondarev, A.A., Dovgodko, E.I., Diachenko, V.A. (2009) Control system for beam scanning in electron beam welding. *The Paton Welding J.*, **9**, 13–16.
7. Skryabinsky, V.V. (1994) *Development of technology of electron beam welding of high-strength aluminium alloys 1570 and 1460 with control of density distribution of beam power*: Syn. of Thesis for Cand. of Techn. Sci. Degree. Kyiv, PWI [in Ukrainian].
8. Lankin, Yu.N., Soloviov, V.G., Semikhin, V.F. et al. (2017) Computer system of graphic design of scanning and modeling of final distribution of electron beam current density. In: *Proc. of 8th Int. Conf. on Beam Technologies in Welding and Materials Processing (11–15 September, 2017, Odessa, Ukraine)*, 59–60.
9. Zhang Hong, Men Zhengxing, Li Jiukai et al. (2018) Numerical simulation of the electron beam welding and post welding heat treatment coupling process. *High Temp. Mater. Proc.*, **37(9–10)**, 793–800.
10. Cerveraa, M., Dialamia, N., Wub, B. et al. (2016) Numerical modeling of the electron beam welding and its experimental validation. *Finite Elements in Analysis and Design*, **121(11)**, 118–133.
11. Lastovirya, V.N. (2008) Principles of control of penetration shape in technological process of electron beam welding. *Mashinostroenie i Inzhenernoe Obrazovanie*, **3**, 12–17 [in Russian].

Received 07.11.2019